J. Physiol. (1972), **227**, *pp.* 173–194
With 10 *text-figures*
Printed in Great Britain

ANALYSIS OF RESPONSES IN VISUAL CELLS OF THE LEECH

By R. FIORAVANTI* and M. G. F. FUORTES

From the Laboratory of Neurophysiology, National Institute of Neurological Diseases and Stroke, National Institutes of Health, Bethesda, Maryland 20014, U.S.A.

(*Received 1 May 1972*)

SUMMARY

1. Potentials were recorded from the cytoplasm and from the vacuole of leech photoreceptors. Since the vacuole is lined with microvilli and is connected to the outside by narrow channels, the potential drops between vacuole and outside measure the current through the microvillar membrane.

2. In darkness, the potential of the cytoplasm with respect to the outside is about -45 mV while the potential of the vacuole is approximately zero.

3. Following illumination the negativity of the cytoplasm decreases and the vacuole becomes negative relative to the outside.

4. For dim intensities, the response to a flash of light may grow proportionately more than the intensity of the flash. This is probably due to development of a depolarizing local response.

5. The resistance from the cytoplasm to the outside was about 150 MΩ in darkness and decreased to approximately 40 MΩ at the peak of the response to a bright flash (on average). Corresponding measurements from the vacuole gave 50 MΩ in darkness and 35 MΩ at the peak of the response.

6. Charging curves produced by steps of constant currents applied to the cytoplasm or to the vacuole include two time constants (about 5 and 50 msec on average). The longer time constant decreases greatly with bright illumination.

7. The results are consistent with the interpretation that the response to light is brought about by an increase of conductance of the microvillar membrane.

* Present address: Laboratorio di Cibernetica e Biofisica, C.N.R. I 16032 Camogli, Italy.

INTRODUCTION

Visual cells of the leech are specially suitable for analysis of the electrical changes associated with responses to light because they offer the possibility to measure the properties of the photosensitive membrane separately from those of the membrane covering other regions of the cell (Lasansky & Fuortes, 1969). In the leech, the specialized microvillar membrane surrounds a large vacuole which is connected to the outside by narrow channels as shown in the diagram of Fig. 1*A*. Since electrodes can be inserted (although not simultaneously) both in the cytoplasm and in the vacuole, it is possible to measure not only the difference of potential between the cytoplasm and the outside, but also between the external fluids in the vicinity of the photosensitive membrane and those surrounding other parts of the cell. This latter measurement gives valuable information on the distribution of the currents produced by light.

THEORY

For purposes of electrical analysis, the visual cell of the leech can be represented by the simple electrical circuit of Fig. 1*B*. In this network g_{12}, c_{12} and e_{12} are respectively the conductance capacitance and (equivalent) electromotive force of the microvillar membrane which separates the cytoplasm (1) from the vacuole (2); g_{13}, c_{13} and e_{13} represent the same quantities in the external membrane and g_{23} is the conductance of the channels connecting the vacuole (2) with the outside (3); v_1 and v_2 are the potentials of the cytoplasm and of the vacuole respectively with reference to the outside.

Surface areas

Estimates of membrane areas are required in order to derive specific values of the electrical parameters. Measurements were taken from optical and electron micrographs and the areas were estimated as follows: The external surface a_{13} is that of a sphere of 30 μm diameter; the area a_{12} of the microvillar membrane is equal to that of its sphere of 16 μm diameter increased by the area of 30 cylinders of 0·1 μm diameter and 1·5 μm height per μm^2. These two areas are

$$a_{12} = 12{\cdot}16 \times 10^{-5} \text{ cm}^2,$$
$$a_{13} = 2{\cdot}83 \times 10^{-5} \text{ cm}^2.$$

The membrane of the axon should be regarded as part of the external membrane. Since the diameter of the axon is only about 1 μm, its space constant will presumably be less than 10^{-2} cm, and therefore the area of axonal membrane within one space constant will be less than 10% of the external soma membrane. Its contributions to the electrical events to be discussed can therefore be disregarded without introducing large errors.

Channels

About the channels it is important to know the cross-sectional area a_s and the length l_s since these two quantities will determine their resistance

$$\frac{1}{g_{23}} = P_{23}\frac{l_s}{a_s},$$

where P_{23} is the resistivity of the material inside the channels. Their values already given by Lasansky & Fuortes (1969) are approximately

$$a_s = 6 \times 10^{-9} \text{ cm}^2; \; l_s = 2 \times 10^{-4} \text{ cm}.$$

Passive membrane properties in darkness and constant illumination

For studies of passive properties, the batteries e_{12} and e_{13} can be disregarded, and the network reduces to the circuit of Fig. 1*C*.

When a current j_1 in the form of a step is applied by means of an electrode in the cytoplasm a charging curve is recorded, having the form

$$\frac{v_1(t)}{j_1} = A_{11}e^{-\alpha_1 t} + A_{12}e^{-\alpha_2 t} + A_{13}, \tag{1}$$

where $A_{11} + A_{12} = -A_{13}$. Similarly, a current j_2 in the vacuole results in the charging curve

$$\frac{v_2(t)}{j_2} = A_{21}e^{-\alpha_1 t} + A_{22}e^{-\alpha_2 t} + A_{23}, \tag{2}$$

where $A_{21} + A_{22} = -A_{23}$.

Using the so-called 'peeling' technique to be described later (see Fig. 5), rough estimates of the six quantities A_{11}, A_{12}, A_{21}, A_{22}, α_1 and α_2 can be derived from these charging curves. Use is then made of the relations

$$A_{11} = \frac{\alpha_1(c_{12}+c_{13}) + g_{12} + g_{13})}{\alpha_1 \gamma}, \tag{3}$$

$$A_{12} = \frac{\alpha_2(c_{12}+c_{13}) + g_{12} + g_{13}}{-\alpha_2 \gamma}, \tag{4}$$

$$A_{21} - \frac{\alpha_1 c_{12} + g_{12} + g_{23}}{-\alpha_2 \gamma}, \tag{5}$$

$$A_{22} = \frac{\alpha_2 c_{12} + g_{12} + g_{23}}{-\alpha_2 \gamma}, \tag{6}$$

$$\alpha_1 = \frac{-\{c_{12}(g_{13}+g_{23}) - c_{13}(g_{12}+g_{23})\} + R}{2c_{12}c_{13}}, \tag{7}$$

$$\alpha_2 = \frac{-\{c_{12}(g_{13}+g_{23}) - c_{13}(g_{12}+g_{23})\} - R}{2c_{12}c_{23}}, \tag{8}$$

where $$\gamma = c_{12}c_{13}(\alpha_1 - \alpha_2)$$

and $$R = \{[c_{12}(g_{13}+g_{23}) + c_{13}(g_{12}+g_{23})]^2 - 4c_{12}c_{13}(g_{12}g_{13} + g_{12}g_{23} + g_{13}g_{23})\}^{\frac{1}{2}}$$

which are derived from the model of Fig. 1*C*, to reach provisional estimates of the parameters of the network. Since there are six independent measurements and five unknowns, the problem can in principle be resolved. The inaccuracy of the data may, however, introduce serious difficulties. In two experiments, a computer fitting procedure (SAAM 25 – Berman, Shahn & Weiss, 1962) was then used, which corrects the initial estimates of the parameters until a satisfactory agreement of calculated and observed data is reached. With other cells, a fit was achieved by simulating the experimental curves on the electrical model of Fig. 1*C*.

The same currents j_1 and j_2, applied during steady-state illumination, produce different charging curves $\bar{v}_1(t)$ and $\bar{v}_2(t)$ from which new values of conductances and capacitances are derived using the same procedures outlined above. In this way all parameters of the model in darkness and during steady-state illumination can be obtained.

Passive membrane properties at the peak of the response to light

The only measurement which can be profitably performed at the peak of a response to a flash of light is the potential drop which is produced by steady-state currents of different intensities (see Fig. 4). Measurements can be performed from the cytoplasm and from the vacuole giving the two input resistances v_1^*/j_1 and v_2^*/j_2. Since the input time constants are short during the response to light, it is assumed that at the peak of the response the potential drops evoked by the currents are already close to their final value. Therefore, the condensers c_{12} and c_{13} are disregarded and the two input resistances are taken as measurements of the conductances of the model at the peak of the response

$$\frac{v_1^*}{j_1} = \frac{g_{12}^* + g_{23}^*}{D^*}, \tag{9}$$

$$\frac{v_2^*}{j_2} = \frac{g_{12}^* + g_{13}^*}{D^*}, \tag{10}$$

where $$D = g_{12}g_{13} + g_{12}g_{23} + g_{13}g_{23}.$$

Having only two measurements for three unknowns, the problem cannot be solved uniquely using these results only. It is necessary, therefore, to assign to the conductance g_{23} the average value determined in darkness or during steady-state illumination by means of experiments in which the whole charging curves were measured. It will be seen that, as expected, the conductance g_{23} of the channels connecting the vacuole to the outside does not vary as a consequence of illumination. Since the three measurements v_1^*/j_1, v_2^*/j_2 and g_{23} are taken from three different and small populations of cells, large errors should be expected in the results obtained with this procedure.

Electromotive forces

Returning to the diagram of Fig. 1*B*, it can now be assumed that the changes produced by light in the voltages v_1 and v_2 are due to changes of the ionic conductances of the membrane. The membrane can then be represented by the circuit of Fig. 1*D*, in which the electromotive forces are given by one inside positive and one inside negative battery. Leaks (conductances not associated with electromotive forces) are disregarded for the sake of simplicity and the capacities are neglected because only slow events are considered. We then have by Thevenin's theorem

$$g = g_n + g_k, \tag{11}$$

$$e = \frac{1}{g}(e_n g_n + e_k g_k), \tag{12}$$

two relations which apply to the branches 12 and 13. Once the conductances g_{12}, g_{13} and g_{23} are known, measurement of the voltages v_1 and v_2 in darkness and during illumination permits one to determine the values of the two voltages e_{12} and e_{13}. When $j = 0$

$$v_1 = \frac{1}{D}\{e_{13}g_{13}(g_{12} + g_{13}) + e_{12}g_{12}g_{13}\}, \tag{13}$$

$$v_2 = \frac{1}{D}(e_{13} - e_{12})g_{12}g_{13}. \tag{14}$$

Knowing the values of v_1 and v_2 (which are measured) and assuming some reasonable values for e_n and e_k, the two conductances g_n and g_k can be determined from eqns. (11) and (12).

METHODS

The leech has five pairs of eyes in its anterior segment. Each consists of a pigment cup covered by a transparent patch of skin and containing about fifty visual cells. Each cell has a large cavity (vacuole) which is surrounded by a microvillar membrane and communicates with the outside through narrow channels (Lasansky & Fuortes, 1969). A diagram of the cell structure is given in Fig. 1. The segment of the mantle containing the eyes was stretched with pins in a paraffin chamber and the skin over the eyes was carefully removed with a razor blade. The exposed visual cells could then be seen under a dissecting microscope. The preparation was covered with Ringer fluid of the following composition: NaCl, 130 mM; KCl, 4 mM; $NaHCO_3$, 2 mM; $CaCl_2$, 2 mM (Nicholls & Kuffler, 1964). Conventional micro-electrode techniques, already described elsewhere (Fuortes, 1959) were employed for recording potentials and for passing currents. The light source was a 30 W tungsten lamp. The light beam covered a circular diaphragm whose reduced image was focused on the eye by means of a low-power microscope objective. A neutral wedge was used to reduce light intensity as desired. The intensity of unattenuated light of wave-length between 4000 and 8000 Å was approximately 10^5 erg cm^{-2} sec^{-1}.

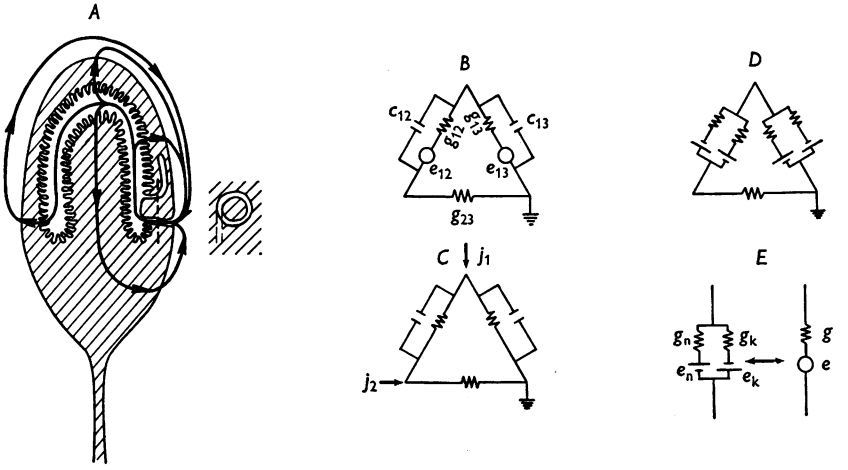

Fig. 1. The structure of the leech photoreceptors is reproduced schematically in *A*. The vacuole is lined with microvilli and communicates with the outside by means of several channels one of which is shown in the diagram (note the appearance of the channel in a cross-section at the level indicated by the dashed line). The width of the channel is 170 Å. The arrows indicate the presumed flow of current during illumination. *B* is the equivalent electrical circuit of the photoreceptor: the branch 13 represents the external membrane, 12 represents the microvillar membrane and 23 is the conductance of the channels. For analysis of the potential drops evoked by extrinsic currents, (j_1 or j_2) the electromotive forces are disregarded and the cell is represented by the circuit in *C*. The diagram in *D* is based on the assumption that two electromotive forces of opposite polarity are associated with the membrane and *E* shows the equivalence (by Thevenin's theorem) of the separate elements in *D* with the combined elements of diagram *B*.

RESULTS

The potential measured upon penetration of the cytoplasm in darkness is about −45 mV, while no appreciable potential change is measured following penetration of the vacuole (Lasansky & Fuortes, 1969). Responses to flashes (illustrated in Fig. 2*A* and *B*) have the general properties already described in preceding papers.

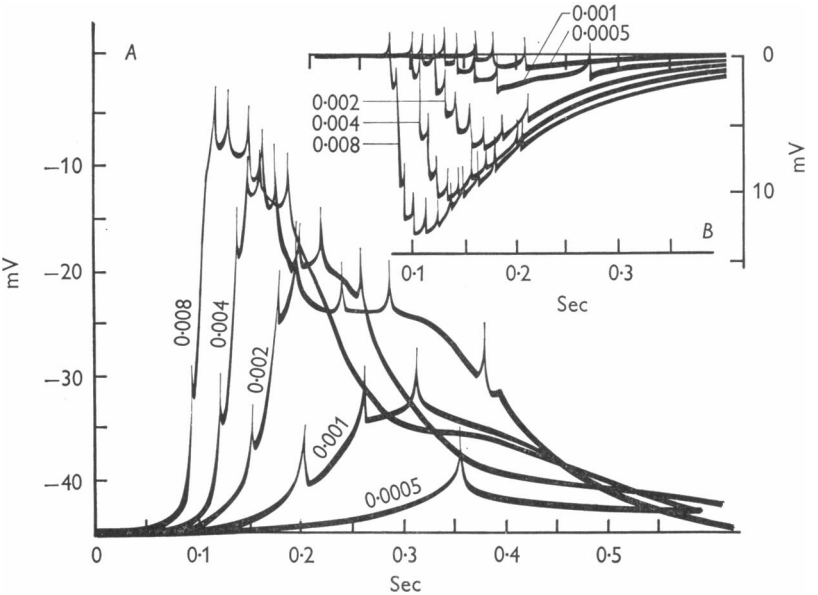

Fig. 2. Responses to flashes of light. In the cytoplasm (*A*) membrane potential in darkness is about −45 mV and the response to light is a positive-going wave. The potential of the vacuole is approximately zero in darkness and flashes of light produce large, negative-going waves, as shown in *B*.

Records *A* and *B* were obtained in different cells. Flash duration was approximately 10 msec in both cases. The figures near each tracing give the intensity of the flash in relative units.

Polarity

During the response to light the cytoplasm develops a positive wave and the vacuole becomes negative with respect to the outside. Thus, current must flow inward through the microvillar membrane and outward through the external membrane, as shown in the diagram of Fig. 1*A*. The spikes superposed on the graded waves have positive polarity both in the cytoplasm and in the vacuole showing that they produce outward current through the microvillar membrane. They must, therefore, be generated at some distance from this site. Since they give small deflexions (5–15 mV) in

the cytoplasm, it is likely that the spike-producing region is in the axon, as it is the case in other cells (Fuortes, Frank & Becker, 1957; Tomita, 1957; Eccles, 1957).

Time course of responses to flashes

As long as the responses of the cytoplasm are small, they have properties similar to those of the visual cells of *Limulus* (Fuortes & Hodgkin, 1964). The time course $v_1(t)$ of responses to dim flashes has the form

$$v_1(t) = Ki\Delta t\, t^n e^{-t/\tau}, \tag{15}$$

where K and τ are constant, n has a value of 5–7 in different cells and $i\Delta t$ is the quantity of light in the flash. In the experiment illustrated (Fig. 3) where the preparation was kept at 22° C, the value of the time constant was $\tau = 53$ msec. The responses to brighter lights deviate sharply from the time course of eqn. (15) as will be described below.

Linearity

It was found in *Limulus* that although the peak and the steady-state amplitude of responses to flashes or steps of light are strongly non-linear with respect to light intensity, their initial phase is simply proportional to the light. This observation shows that the non-linearities follow the initial development of the response and have been interpreted assuming that they are brought about by a feed-back which decreases the sensitivity of the system as the response increases (Fuortes & Hodgkin, 1964). Initial linearity is observed also in the responses of the leech visual cells as can be demonstrated by the procedure illustrated in Fig. 3: after fitting expression (15) to the responses to dim flashes, the theoretical curves are traced for brighter lights and superposed to the corresponding experimental responses, as shown in Fig. 3*A*. In this experiment the responses follow the theoretical curves for the major part of their duration for flashes of less than 0·004 units of intensity. With brighter flashes the theoretical and experimental curves coincide only at the very start (up to voltage changes of about 5 mV), as it is the case in *Limulus*, but then they deviate sharply. The discrepancy reveals features which differ from those observed in other preparations: in *Limulus*, as soon as the linear range is exceeded, the experimental responses are at all times smaller than the theoretical curves (except for the possible presence of a sharp, spike-like transient). In the leech instead, they may be conspicuously larger. In the experiment of Fig. 3, the response to the flash of intensity 0·004 is larger than the theoretical curve throughout its time course (except at the very beginning). With brighter lights the response is initially larger and later smaller than the theoretical responses. There may be, therefore, in the cell mechanisms

producing amplification, perhaps similar to the mechanisms which produce fast transients in other photoreceptors. Subtraction of the theoretical from the experimental response gives the excess produced by these amplifying mechanisms. The waves resulting from such subtractions are shown at the bottom of Fig. 3*A*.

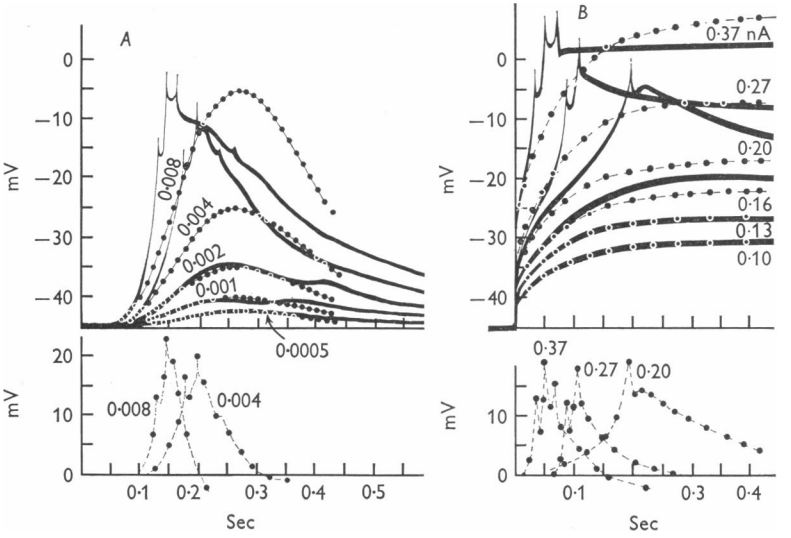

Fig. 3. Local responses of photoreceptors.

A: responses to flashes recorded from the cytoplasm as in Fig. 2*A*. The dashed lines are theoretical curves defined by eqn. (15) with $n = 5$, and $\tau_1 = 53$ msec.* The light intensity i is given by the figures near each trace. The first three responses fit roughly the dashed lines but the other responses are transiently larger. The excess of the experimental response over the theoretical (linear) curves is plotted in the lower section of the Figure.

B: charging curves produced by steps of depolarizing curves in the same cell. Current intensity shown near each trace. The dashed lines are the charging curves which would be obtained if the responses were linear. It is seen instead that intensities greater than $1{\cdot}3 \times 10^{-10}$ A evoke additional depolarizing waves, due to which the experimental curves transiently exceed the linear responses given by the dashed lines. Subtraction of the linear from the experimental responses gives the curves in the lower section, which are roughly similar to the curves obtained by subtraction in the responses to flashes of light.

* (Note that the parameter n in this expression corresponds to $n-1$ in the formulae given by Fuortes & Hodgkin, 1964).

Depolarizing local responses

In *Limulus*, depolarizing waves may be produced by means of electric currents, most easily just after the end of a hyperpolarizing pulse but in favourable conditions also at the start of a depolarizing current pulse (see Baumann, 1968 for similar results on the honeybee). Depolarizing waves are produced by currents also in the visual cells of the leech. Fig. 3*B* shows responses to depolarizing steps of increasing intensity in the same cell of Fig. 3*A*: weak currents produce charging curves described by eqn. (1) but the response to stronger currents may include an additional depolarizing wave. Subtraction of the expected charging curves from these more complex responses (bottom) leaves waves which are not unlike those obtained when a similar subtraction is applied to the responses to flashes of light. This suggests that the transients of Fig. 3 are a local response which develops when the membrane is appropriately depolarized.

Relation of the responses of the cytoplasm and of the vacuole

The peak height of responses to flashes recorded from the cytoplasm and from the vacuole was plotted as a function of the logarithm of light intensity in twenty-one experiments. The points obtained in the different experiments presented a wide scatter even after normalizing the data to the same maximal height. Scatter was reduced, however, by slight adjustment of the light-intensity scale, a procedure which may be justified since individual differences in sensitivity would be expected to occur in different preparations or as a consequence of different states of adaptation. With this adjustment (which never exceeded a factor of two) average curves could be fitted to the data, giving the results of Fig. 4. The most important feature of this plot is that during the response to bright light, the voltage of the vacuole is negative with respect to the cytoplasm. As already stated the current produced by the response flows from the outside fluids to the vacuole and from there into the cytoplasm. This current, therefore, tends to make the cytoplasm negative to the vacuole. Since the opposite occurs, there must be in the branch 12 a positive battery. Therefore, during the response to a bright light, the battery e_{12} must have its positive pole toward node 1.

In the average data of Fig. 4, the growth of the response with light intensity follows a somewhat different course in the cytoplasm or in the vacuole. The difference, however, is not very great and could be due to the variability of the properties of individual cells.

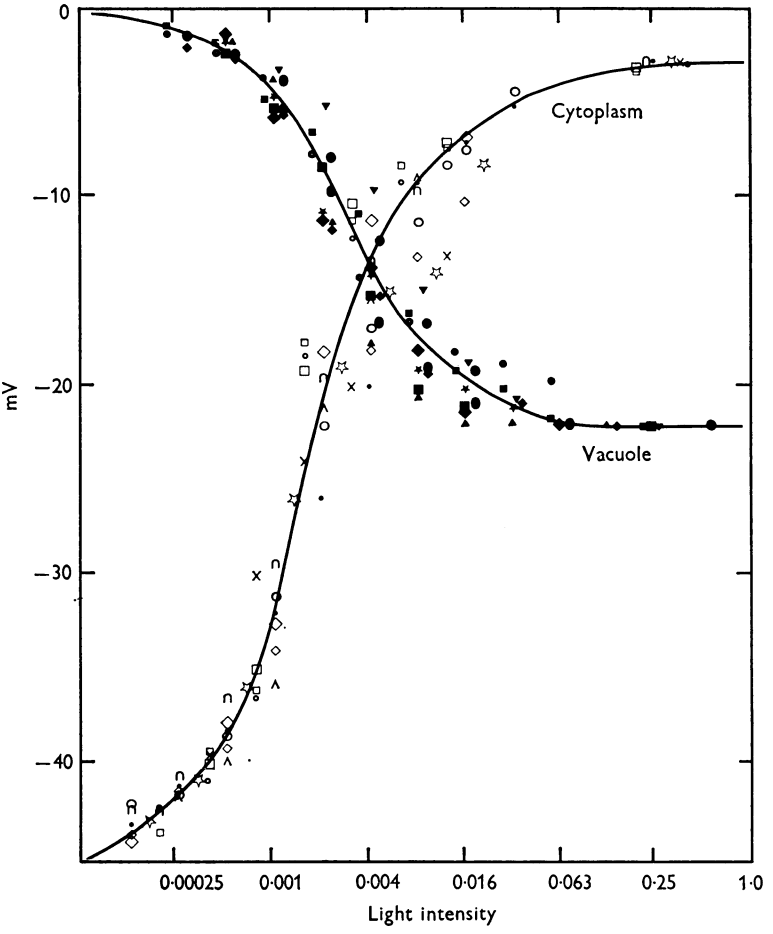

Fig. 4. Relation between light intensity and response of cytoplasm and of vacuole. Peak height of responses evoked by flashes of different intensities were recorded from the cytoplasm in eleven units and from the vacuole in ten units. Response amplitude was normalized based on the average peak height of the response to a flash of unit intensity (42·1 mV in the cytoplasm and −22 mV in the vacuole). Average potentials in darkness were −45 mV in cytoplasm and zero in the vacuole. Individual plots were shifted on the horizontal axis to compensate for variations in the sensitivity to light of different units. Measurements from the cytoplasm are shown by open symbols, those from the vacuole by filled symbols. The crossing of the curves through the points shows that, during the response to bright flashes, the vacuole becomes negative with respect to the cytoplasm.

Resistance measurements in darkness

The potential drops evoked by currents j_1 through the cytoplasm in darkness are illustrated in Fig. 5*A*. These curves consist of two phases: a rapid initial step followed by a much slower charge to the final level. When the logarithm of the voltage drop is plotted as a function of time (Fig. 5*B*), a curve is obtained in which the late measurements can be fitted by a straight line which intercepts the ordinate at the voltage A_{12} and has the slope $-\alpha_2$. This line is then the semi-logarithmic plot of the expression

$$v = A_{12}e^{-\alpha_2 t}.$$

The early points are now subtracted from the straight line ('peeling' procedure) and replotted as before giving another straight line with intercept A_{11} and slope $-\alpha_1$.

In some experiments the electrode originally inserted in the cytoplasm moved spontaneously into a vacuole which was then presumed to be the vacuole of the same cell. In these cases, a new charging curve could be recorded (Fig. 6) from which the voltages A_{21} and A_{22} could be determined using the technique just described. Conductances and capacitances were then computed from formulae (3) to (8) and their values were corrected by the computer program mentioned before. The accuracy of the fit between calculated and observed data is shown for one experiment in Fig. 7. When the fit was obtained by simulation with the electrical model of Fig. 1*C*, the same procedure was used to obtain initial estimates of the parameters. In order to correct these estimates so as to achieve satisfactory coincidence of the two curves, it is useful to keep in mind that the initial slope of the charging curve $v_1(t)/j_1$ is controlled by c_{13}; its final value is determined predominantly by the quantity $g_{12}+g_{13}$ and the final value of $v_2(t)/j_1$ is given almost exclusively by the conductance g_{23}. An example of the fit obtained in this way is given in Fig. 8.

The parameters of the model were determined in this manner in fourteen cells. Only for nine of these units, however, were results available both in light and in darkness.

The values found with both fitting procedures are summarized in Table 1, from which the following conclusions emerge. In darkness, the conductance g_{12} is about one fifth of g_{13} and one tenth of g_{23}; the resistivity ρ_{13} of the external membrane is similar to that of other nervous structures but the resistivity ρ_{12} of the microvillar membrane is unusually high. About fifty-fold higher than in the squid axon (see Millecchia & Mauro, 1969 and Brown, Hagiwara, Koike & Meech, 1970 for similarly high resistivities in other photoreceptors). In contrast with the resistivities, the specific capacities of the two membranes are similar to each other but about twice

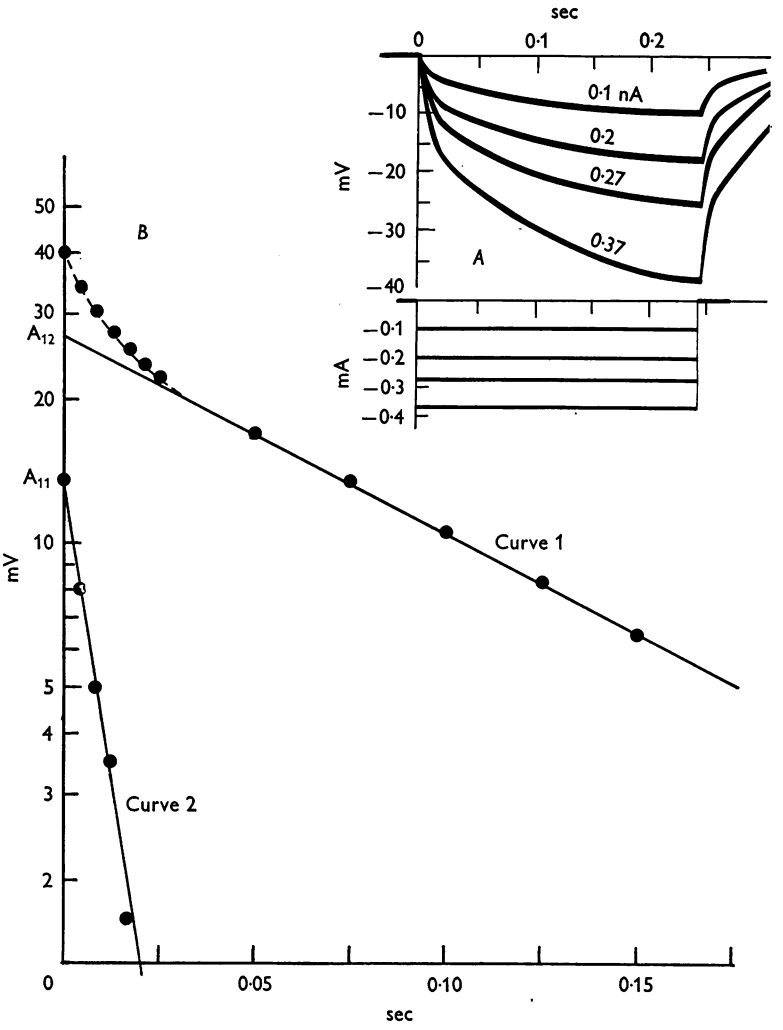

Fig. 5. Responses of the cytoplasm to extrinsic currents. *A*: charging curves recorded from the cytoplasm following steps of constant current. Current steps monitored by the lower traces. Current intensities shown by the figures near each charging curve. The responses are roughly linear with respect to current intensity. Curve 1 in *B* is a semilogarithmic plot of the difference between the last charging curve (3·7) and its asymptotic value (−40 mV). The straight line through the points has slope $-\alpha_2$ and its intercept with the ordinate is a measure of the quantity A_{12} in eqn. (1). Subtraction of this straight line from the points which remain above it (peeling) gives curve 2, with slope $-\alpha_1$ and intercept A_{11}.

as large as in the squid axon and in other membranes. This could be due in part to errors in the estimates of areas.

During bright constant illumination g_{12} increases about sixteenfold while all other parameters show only minor changes, well within the limits of error.

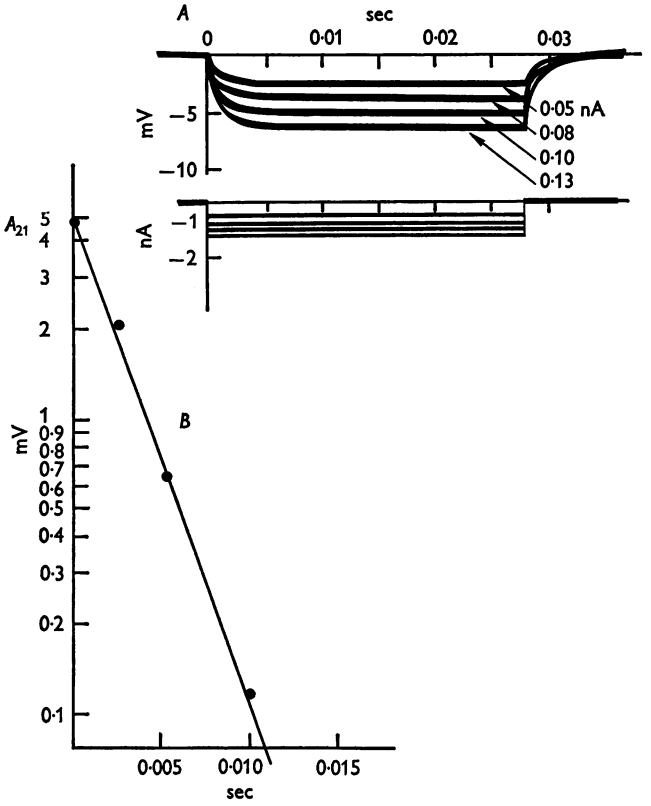

Fig. 6. Charging curves recorded from the vacuole. *A* shows tracings of experimental responses to steps of constant current applied through a micro-electrode in the vacuole. Current intensities (shown by the bottom traces) are indicated by the figures at right. The semi-logarithmic plot in *B* was obtained as in Fig. 5. The line through the points has a slope $-\alpha_1$. The deflexion associated with the long time constant α_2 is too small to be resolved.

The standard deviation from the mean was about $\pm 50\,\%$ for all parameters with variations from cell to cell in excess of a ratio 1:5. This is not surprising considering the expected variability of the size of individual cells, variability of structure (such as relative size of the vacuole and number of channels), experimental damage and errors in measurement.

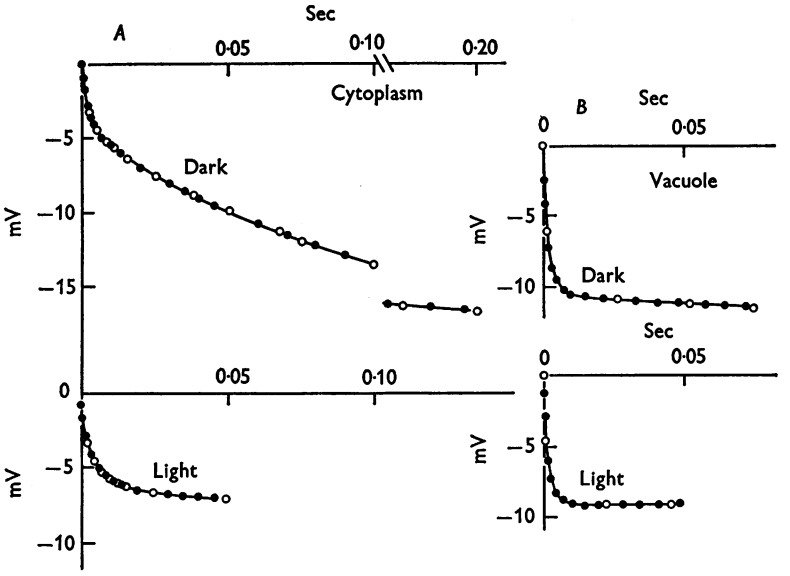

Fig. 7. Computer fit of charging curves. Using the procedure described in the text, the computer program SAAM 25 adjusts the values of the electrical parameters of Fig. 1*C* until a good fit is obtained between experimental and computed charging curves. *A* shows the charging curves of the cytoplasm in darkness (above) and during bright, constant illumination (below). Corresponding results in the vacuole are illustrated in *B*. Open circles are experimental and filled circles are computed points.

Measurements at the peak of the response to a flash

Input resistances at the peak of the response to a flash are estimated by measuring the potential drops evoked by steady currents on the transients recorded from the cytoplasm and from the vacuole respectively (Figs. 9 and 10). The average values of these potential drops for twenty cells were:

$$\frac{v_1^*}{j_1} = 39{\cdot}0 \times 10^6\,\Omega,$$

$$\frac{v_2^*}{j_2} = 35{\cdot}5 \times 10^6\,\Omega.$$

It was clear in all experiments that the input resistance from the cytoplasm drops greatly at the peak of the response becoming then similar to the resistance measured from the vacuole. Since

$$r = \frac{v_1/j_1}{v_2/j_2} = \frac{g_{12}+g_{13}}{g_{12}+g_{23}}$$

the observation that r is close to unit implies either that g_{13} and g_{23} are

similar, or that g_{12} is large in comparison with both g_{13} and g_{23}. Taking the average value determined in other experiments $g_{23} = 1{\cdot}842 \times 10^{-8}$ mho, we obtain $g_{12} = 10{\cdot}7 \times 10^{-8}$ mho and $g_{13} = 1{\cdot}30 \times 10^{-8}$ mho. Even though the quantitative results, depending critically on the measurements, are not very reliable, it seems safe to conclude that the major change occurring at the peak of the response to a bright flash is a large increase of the conductance g_{12}.

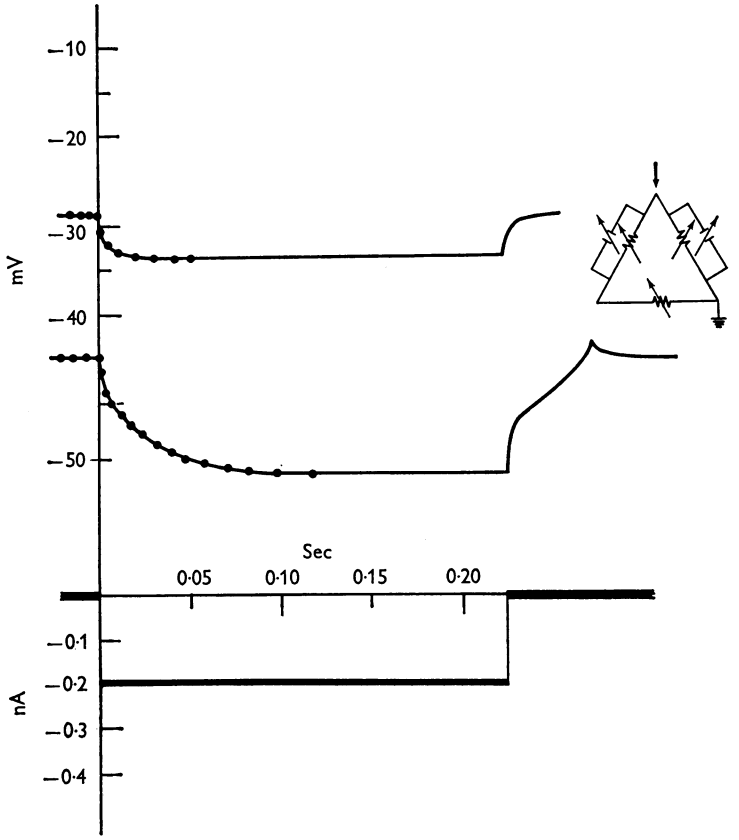

Fig. 8. Simulation of responses to currents. The variable resistances and condensers in the network at right are adjusted until the voltage drop $v_1(t)$ produced by a step of constant current j_1 has the same shape as the experimental charging curves. The continuous lines are tracings of responses of the cytoplasm to steps of current applied during bright illumination (top) or in darkness. The filled circles are points on the charging curve of the electrical network. The same procedure was applied to the responses recorded from the vacuole. In this way, the values of the electrical parameters which fit the experimental measurement are determined directly.

TABLE 1. Shows the values of the electrical components of the network of Fig. 1*C*, which result in charging curves similar to those recorded from fourteen visual cells. The fits were obtained either by computation (Fig. 7) or by simulation (Fig. 8) as explained in text. The column headings D and L denote dark and steady light respectively. The three bottom rows give average, S.D. and fractional S.D. of each row. The average input resistances v_1/j_1 and v_2/j_2 were much larger in this group of cells than in the smaller group described in a previous article (Lasansky & Fuortes, 1969). The reasons for this quantitative discrepancy are not known

	mhos × 10^{-8}						$F \times 10^{-10}$			
	g_{12}		g_{13}		g_{23}		c_{12}		c_{13}	
Cell	D	L	D	L	D	L	D	L	D	L
1	0·073	0·9	0·42	0·53	0·80	0·9	2·4	2·8	0·40	0·40
2	0·102	3·95	0·39	0·55	0·65	0·6	2·43	2·0	0·45	0·45
3	0·266	3·3	0·319	0·318	1·78	1·75	4·58	3·3	0·46	0·46
4	0·230	5·28	1·26	1·26	1·90	1·9	2·0	2·0	0·50	0·50
5	0·346	5·9	1·3	1·3	5·9	5·9	2·94	2·94	0·59	0·59
6	0·101	1·55	0·53	0·61	1·5	1·1	3·8	2·9	0·48	0·48
7	0·210	2·0	2·0	2·0	1·0	1·0	3·2	2·7	0·32	0·30
8	0·106	0·40	1·0	1·0	1·4	1·45	3·0	3·0	0·25	0·25
9	0·33	2·7	1·8	2·0	1·85	2·7	9·3	7·3	0·91	0·91
10	0·266	—	0·319	—	1·78	—	4·58	—	0·46	—
11	0·073	—	0·42	—	0·80	—	2·4	—	0·40	—
12	0·23	—	1·26	—	1·90	—	2·0	—	0·50	—
13	0·23	—	1·26	—	1·90	—	2·0	—	0·50	—
14	0·23	—	1·26	—	1·90	—	2·0	—	0·50	—
Ave.	0·200	2·89	0·986	1·04	1·79	1·92	3·33	3·22	0·48	0·48
S.D.	0·089	1·79	0·530	0·615	1·22	1·53	1·87	1·5	0·14	0·18
F.S.D.	0·446	0·619	0·537	0·591	0·682	0·797	0·562	0·466	0·292	0·375

	sec × 10^{-3}				Ω × 10^8			
	τ_{12}		τ_{13}		v_1/j_1		v_2/j_2	
Cell	D	L	D	L	D	L	D	L
1	330	31·1	9·6	7·6	2·05	1·02	1·16	0·813
2	238	5·1	11·4	8·2	2·09	0·934	1·37	0·923
3	172	10·0	14·3	14·3	1·82	0·684	0·519	0·490
4	87	3·79	3·96	3·96	0·683	0·376	0·478	0·343
5	85	4·98	4·54	4·54	0·615	0·235	0·162	0·144
6	376	18·7	9·06	7·87	1·6	0·798	0·631	0·650
7	152	13·5	1·6	1·5	0·46	0·375	0·840	0·5
8	283	75·0	2·5	2·5	0·910	0·761	0·669	0·576
9	281	27·0	5·06	4·55	0·481	0·299	0·470	0·260
10	172	—	14·4	—	1·82	—	0·519	—
11	32·9	—	9·52	—	2·05	—	1·16	—
12	86·9	—	3·97	—	0·683	—	0·477	—
13	86·9	—	3·97	—	0·683	—	0·477	—
14	86·9	—	3·97	—	0·683	—	0·477	—
Ave.	198	21·0	6·99	5·56	1·19	0·604	0·669	0·522
S.D.	103	21·2	4·15	3·73	0·64	0·281	0·330	0·288
F.S.D.	0·519	1·02	0·594	0·671	0·539	0·465	0·493	0·456

Electromotive forces

Taking the values of g_{12}, g_{13} and g_{23} determined in darkness, during a steady illumination and at the peak of the response to a flash, the electromotive forces e_{12} and e_{13} in Fig. 1*B* can be estimated for the same three conditions, making use of eqns. (13) and (14). In darkness $v_2 = 0$ and, therefore, from eqn. (14) $e_{13} = e_{12}$. Knowing that $v_1 = -45$ mV, substitution of the numerical values of the conductances in eqn. (14) gives $e_{12} = e_{13} = -48{\cdot}3$ mV. During constant bright illumination, the response of the cytoplasm decays by about one half of its initial peak value, while the response of the vacuole decays by an even larger fraction. Average values in the same cells of Table 1 were: $\bar{v}_1 = -32$ mV; $\bar{v}_2 = -6$ mV, and from these values we obtain:

$$\bar{e}_{12} = -29{\cdot}9 \text{ mV}; \quad \bar{e}_{13} = -50{\cdot}7 \text{ mV}.$$

Finally, at the peak of the response to a bright flash, the potential of the cytoplasm is close to zero ($v_1^* = -3$ mV, as the average of twelve cells) while the vacuole becomes strongly negative ($v_2^* = -22$ mV, as the average of twelve cells). It follows from these data that,

$$e_{12}^* = +27{\cdot}1 \text{ mV}; \quad e_{13}^* = -29{\cdot}7 \text{ mV}.$$

Ionic conductances

It is reasonable to assume at this point that the two branches e_{12}, g_{12} and e_{13}, g_{13} in Fig. 1*B* are Theverin equivalents as explained in a previous section (see Fig. 1*E*). It will be further assumed that e_n and e_k represent electromotive forces given by sodium and potassium concentration gradients respectively, and that their values are

$$e_n = +40 \text{ mV}; \quad e_k = -80 \text{ mV}.$$

With these assumptions, the values of g_n and g_k can be determined from eqns. (10) and (11), making use of the estimates given above for g_{12}, e_{12}, g_{13} and e_{13}. These values are given in Table 2 for the three situations, darkness, constant light, and peak of the response to a flash.

In spite of the many uncertainties attached to these results, it seems clear that light produces a large increase of the conductance g_{12} of the microvillar membrane and that, at the peak of the response to light, the equivalent electromotive force e_{12} associated with this conductance changes from negative to positive.

In order to fit the measurements performed at the peak of the response, it was also necessary to increase the conductance g_{13} and to decrease the negative voltage e_{13}, and this was satisfactorily accomplished by a moderate

increase of the 'sodium' conductance $g_{n(13)}$. Given the large scatter of the data which led to Table 2, however, it is difficult to regard this inference as reliable.

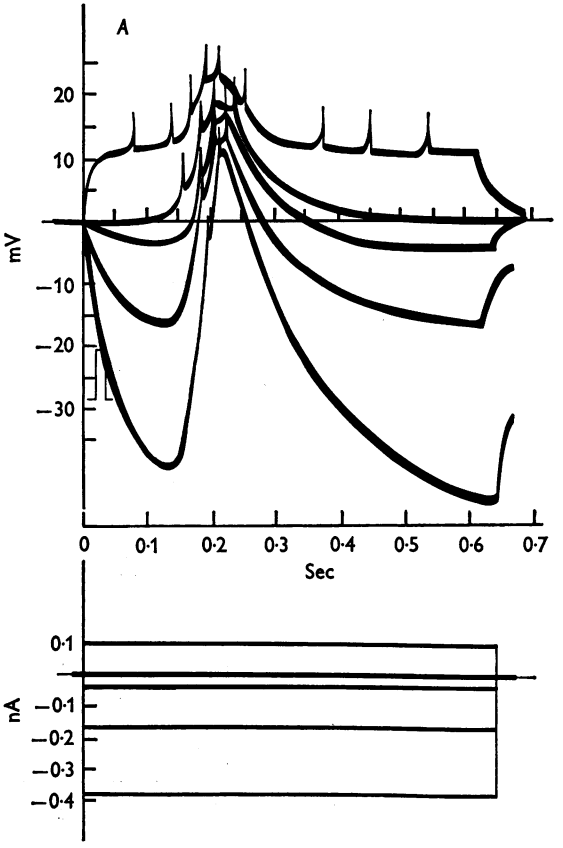

Fig. 9A. For legend see opposite page.

DISCUSSION

All visual cells possess a specialized membrane which is characterized by infoldings and contains the visual pigment. With the exception of the vertebrate rods, the photoreceptive area of the membrane is attached to a smooth membrane showing no signs of specialization. In most cases, therefore, the electrical measurements which can be performed reflect the properties of both the photoreceptive and the non-specialized membrane, a situation which makes it difficult to determine how each area contributes to the visual response.

In the visual cells of the leech, instead, it is possible to record not only the potentials between the inside and the outside of the cell, but also the

currents through the microvillar membrane. A sufficient number of measurements can then be taken to determine separately the characteristics of the two membranes and the changes produced in them by illumination. Unfortunately it was not possible in this study to record currents and potentials simultaneously from the same cell. Therefore, the two measurements had to be taken separately, in a few cases from the same cell but at different times, and in the majority of cases from different cells.

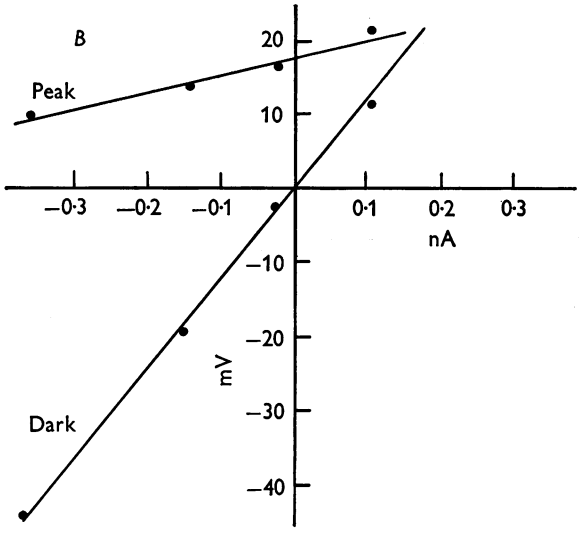

Fig. 9. Effect of currents on the responses of the cytoplasm to flashes.

A: responses to flashes of intensity 0·008 were recorded from the cytoplasm while currents of different intensities were applied through the micro-electrode. The flash was delivered just after the start of the current step, as indicated.

B: same data as in *A*. The points measure the potentials at the end of the current pulse and at the peak of the response to the flash. The slopes of the lines through the points are regarded as measurement of resistance in darkness and at the peak of the response. Taking the data before the charging curve has reached its steady state introduces appreciable errors. Resistance measurements must therefore be regarded as only very approximate.

TABLE 2. Values of capacitance and electromotive force in differing conditions of light.

	Branch 12					Branch 13				
	g	e	g_n	g_k	g_n/g_k	g	e	g_n	g_k	g_n/g_k
Dark	0·1995	−48·3	0·0526	0·1469	0·3584	1·005	−48·3	0·2652	0·7398	0·3584
Steady light	2·90	−29·9	1·2177	1·6883	0·7177	1·005	−50·7	0·2456	0·7594	0·3235
Peak	10·70	+27·1	9·5646	1·1514	8·3066	1·30	−29·7	0·5444	0·7576	0·7205

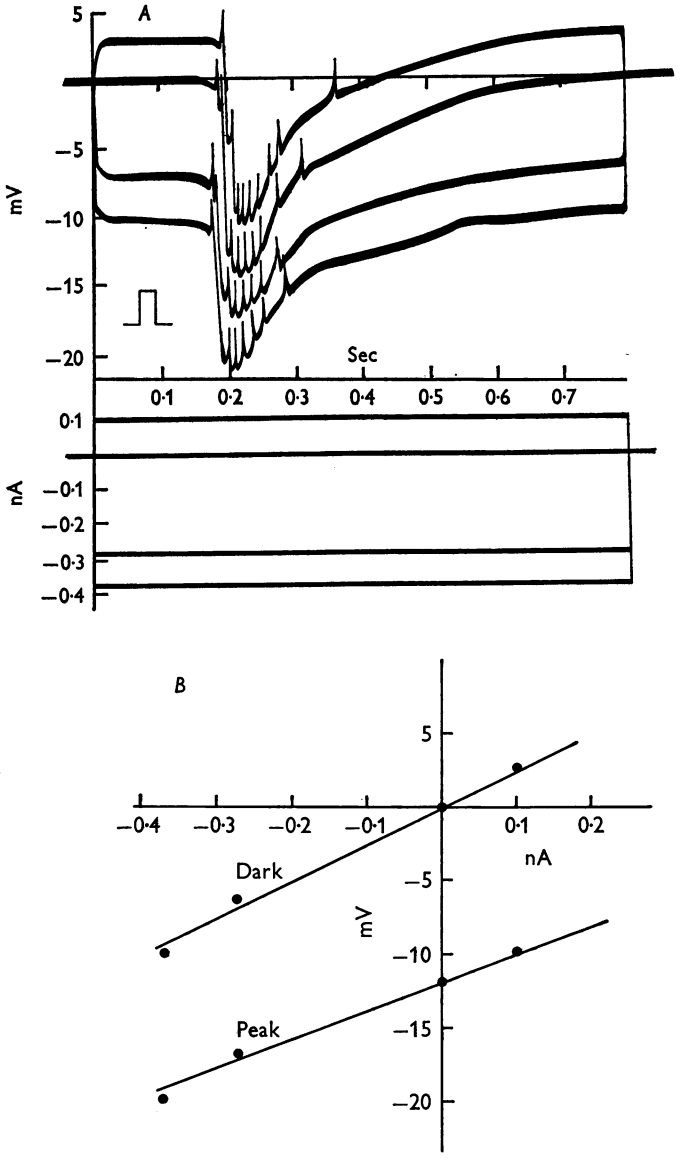

Fig. 10. Effects of currents on the responses of the vacuole. Same experiment as in Fig. 9 but with the electrode in the vacuole. Flash intensity 0·016.

It turned out that, for each measurement, the range of variation in individual cells exceeded the ratio of 1:5 with consequent large uncertainty in the average values. In these conditions the quantitative results must be regarded as unreliable, especially when the values of the unknown parameters depend critically upon the values of the data.

A number of qualitative conclusions seems, however, to be fairly well established: (1) the observation that the potential of the vacuole is zero in the dark and becomes negative with light indicates that no current flows through the microvillar membrane during darkness and that an inward current develops as a consequence of illumination; (2) the inward photocurrent is associated with a large increase of the microvillar membrane conductance. This conclusion is derived from the analysis of the charging curves. It can be readily seen that it is consistent with the finding that the resistance and time constants measured from the cytoplasm and from the vacuole become very similar following illumination, since high conductance of the microvillar membrane approximates a short-circuit between cytoplasm and vacuole. The calculated conductance increase was 14·5-fold in the steady state and 50-fold at the peak of the response to a bright light. In both conditions the changes are too large to be ascribed to experimental errors or to statistical variability; (3) conversely, the calculated conductance changes brought about by light in the external membrane and in the channels are small and probably within the range of experimental error. This leads to the conclusion that, if these conductances are altered at all following illumination their changes are much less than at the microvillar membrane; (4) membrane capacity would not be expected to change with activity. For this reason it was satisfactory to find that, although all parameters in the model were adjusted independently to give best fit with the data, the calculated capacities were not appreciably altered by illumination; (5) the observation that the vacuole becomes negative with respect to both the cytoplasm and the outside at the peak of the response to a bright light indicates that a cytoplasm-positive electromotive force must be associated with the microvillar membrane at the peak of the response. This in turn suggests that this membrane becomes selectively permeable to sodium ions following bright illumination.

The interpretation proposed some time ago (Fuortes, 1959; Rushton, 1959) that the depolarizing generator potentials of visual cells are brought about by a conductance change of the cell membrane seem, therefore, to be in good agreement with the results obtained in the leech.

We wish to thank Dr T. R. Colburn of the National Institute of Mental Health for his valuable help in the analysis of the electrical circuits discussed in this article.

REFERENCES

BAUMANN, F. (1968). Slow and spike potentials recorded from the retinular cells in the honeybee drone in response to light. *J. gen. Physiol.* **52**, 855–875.

BERMAN, M., SHAHN, E. & WEISS, M. F. (1962). The routine fitting of kinetic data to models. *Biophys. J.* **2**, 275–287.

BROWN, H. M., HAGIWARA, S., KOIKE, M. & MEECH, R. M. (1970). Membrane properties of Barnacle photoreceptor examined by the voltage-clamp technique. *J. Physiol.* **208**, 385–413.

ECCLES, J. C. (1957). *The Physiology of Nerve Cells.* Baltimore: The Johns Hopkins Press.

FUORTES, M. G. F. (1959). Initiation of impulses in visual cells of *Limulus*. *J Physiol.* **148**, 14–28.

FUORTES, M. G. F., FRANK, K. & BECKER, M. C. (1957). Steps in the production of motoneuron spikes. *J. gen. Physiol.* **40**, 735–752.

FUORTES, M. G. F. & HODGKIN, A. L. (1964). Changes in time scale and sensitivity in the ommatidia of *Limulus*. *J. Physiol.* **172**, 239–263.

LASANSKY, A. & FUORTES, M. G. F. (1969). The site of origin of electrical responses of visual cells of the leech, *Hirudo medicinalis*. *J. cell Biol.* **42**, 241–252.

MILLECCHIA, R. & MAURO, A. (1969). The ventral photoreceptor cells of Limulus. *J. gen. Physiol.* **45**, 310–330.

NICHOLLS, J. G. & KUFFLER, S. W. (1964). Extracellular space as a pathway for exchange between blood and neurons in the central nervous system of the leech: ionic composition of glial cells and neurons. *J. Neurophysiol.* **27**, 645–671.

RUSHTON, W. A. H. (1959). A theoretical treatment of Fuortes's observations upon eccentric cell activity in *Limulus*. *J. Physiol.* **148**, 29–38.

TOMITA, T. (1957). Peripheral mechanism of nervous activity in lateral eye of horseshoe crab. *J. Neurophysiol.* **20**, 245–254.